JCTC Journal of Chemical Theory and Computation

Applications of Screened Hybrid Density Functionals with Empirical Dispersion Corrections to Rare Gas Dimers and Solids

Kazim E. Yousaf and Edward N. Brothers*

Science Program, Texas A&M at Qatar, Texas A&M Engineering Building, Education City, Doha, Qatar

Received October 11, 2009

Abstract: An empirical dispersion correction is added to the range-separated hybrid density functionals HSE and HISS via parametrization versus a standard test bed of weakly bound complexes. The performance of the resulting HSE-D and HISS-D functionals is evaluated by calculating the equilibrium bond length, harmonic frequency, and dissociation energy for a number of rare gas dimers, and the lattice constants, band gaps, and sublimation energies of the rare gas solids. Both HSE-D and HISS-D are shown to provide accurate results for both molecules and extended systems, suggesting that the combination of a screened hybrid functional with an empirical dispersion correction provides an accurate, widely applicable method for use in solid-state and gas-phase electronic structure theory.

1. Introduction

Kohn−Sham density functional theory[1] (KS-DFT) continues to be a hugely popular and successful electronic structure method for a number of reasons. With modern functionals, DFT offers the tantalizing combination of accurate results at a fraction of the computational cost required for a correlated ab initio calculation. Many of today's most useful functionals belong to the class of so-called hybrid functionals, mixing a fraction of (nonlocal) Hartree−Fock exchange with conventional local exchange functionals. Hybrid functionals offer significant improvements in accuracy over those not containing exact exchange and must be used to obtain even qualitatively correct results for a number of properties of both molecules and solids. This presents a problem in the case of the latter, however, because exact exchange exhibits slow spatial decay, and, as such, traditional hybrid DFT calculations on solids are generally unfeasible. In addition, many functionals (especially older functionals) have difficulty with molecular and periodic systems in which dispersion interactions play an important role. Such interactions are known to arise from long-range electron correlations, which are inadequately modeled by the majority of functionals.

Attempts have been made, in recent years, to overcome both of these issues. In range-separated hybrid functionals, the Coulomb operator is partitioned into two or more distance ranges, and with appropriate parametrization the fraction of exact exchange included is allowed to vary as a function of interelectronic separation r_{12}. The functional of Heyd, Scuseria, and Ernzernhof[2,3] (HSE, also known as HSE06) is an early example of such a functional and was designed to include exact exchange only at small r_{12}, thus ameliorating the computational expense of modeling solids. HSE is among the most accurate density functionals for band gap calculations in solids due to this short-range Hartree−Fock exchange and has also been shown to yield good structural and energetic data for extended systems.[4−7] However, its performance in molecular calculations is not as impressive because the exchange potential now lacks the correct asymptotic behavior. The LC-ωPBE functional[8,9] is designed in a similar way to HSE but, conversely, includes only long-range exact exchange. This functional consequently outperforms HSE for many molecular properties, but is unsuitable for calculations on extended systems. Henderson, Izmaylov, Scuseria, and Savin (HISS) developed a functional[10] in an attempt to combine the best features of the HSE functional in calculations on solids with those of the LC-ωPBE functional in molecular calculations. In the HISS functional,

* Corresponding author e-mail: ed.brothers@qatar.tamu.edu.

10.1021/ct900536n
Published on Web 02/11/2010

the Coulomb operator is split not only into short-range and long-range components, as in HSE and LC-ωPBE, but also into a middle-range part. HISS is parametrized so that exact exchange is only computed in this middle r_{12} range and has been shown to give only slightly less accurate results on solids than HSE, while yielding far superior accuracy for finite systems.[11]

Regardless of the importance of exact exchange, however, it cannot improve the description of a system in which dispersion interactions are important. Many different solutions to this problem have been proposed, but in this work we focus on the popular empirical dispersion correction of Grimme, commonly known as the DFT-D method.[12,13] In this conceptually simple approach, a pairwise empirical correction, which depends on a single, optimized functional-dependent scaling parameter, is added to the KS-DFT energy. There are obvious limitations to this approach, as a semiempirical correction can only improve an already a reasonable semilocal interaction curve, and not all dispersion interactions are pairwise.[14] However, this correction is extremely quick to calculate as compared to the self-consistent field step of a KS-DFT calculation, even for large systems, and DFT-D has yielded excellent geometries and interaction energies for dispersion bound complexes.[12,13] Recently, the DFT-D method has been extended to the domain of solid-state electronic structure calculations by a number of groups with encouraging results.[15−17]

By combining a screened hybrid functional with an empirical dispersion correction, it is hoped that an accurate universal functional that could be applied to both molecules and solids could be constructed. In the present study, optimal s_6 values are determined for the HSE and HISS functionals against a standard set of weakly bound complexes, and the performance of the resultant HSE-D and HISS-D functionals is assessed by calculating the geometry, harmonic frequency, and dissociation energy for a number of rare gas dimers. With our implementation of DFT-D under periodic boundary conditions, these functionals are then used to calculate the lattice parameters, sublimation energies, and band gaps of the dispersion bound rare gas solids. Note that these systems are vastly different from those in our training set and were selected to demonstrate the transferability of our parametrization and general applicability of our corrected functionals.

2. Theory

2.1. Range-Separated Hybrid Density Functionals. A recent overview of the theory and applications of range-separated hybrids was given by Henderson et al.;[18] the interested reader is referred to this paper, but a brief summary is given here for the sake of convenience. Following the ideas of Savin,[19,20] in this type of functional the Coulomb operator r_{12}^{-1} is typically partitioned into a short-range and a long-range component:

$$\frac{1}{r_{12}} = \frac{\mathrm{erfc}(\omega r_{12})}{r_{12}} + \frac{\mathrm{erf}(\omega r_{12})}{r_{12}} \tag{1}$$

where the first and second terms on the right-hand side contain the short- and long-range (SR and LR) parts of the exchange, respectively, the complementary error function is defined as $\mathrm{erfc}(\omega r) = 1 - \mathrm{erf}(\omega r)$, and ω is an adjustable parameter that controls the definition of the two ranges. In the Heyd−Scuseria−Ernzerhof (HSE) screened hybrid functional, the first of these range-separated hybrids considered in this work, $\omega = 0.11\ a_0^{-1}$. The error function is not the only suitable function for use in this partitioning, but has the desirable property that the requisite integrals are easy to calculate analytically. HSE is based on the PBE0 hybrid functional,[21,22] and the HSE exchange-correlation energy is given by

$$E_{\mathrm{xc}}^{\mathrm{HSE}} = E_{\mathrm{xc}}^{\mathrm{PBE}} + \frac{1}{4}(E_{\mathrm{x}}^{\mathrm{HF,SR}} - E_{\mathrm{x}}^{\mathrm{PBE,SR}}) \tag{2}$$

with the mixing coeffecient 1/4 obtained from perturbation theory.[23] HSE is thus equivalent to PBE0 for $\omega = 0$ and approaches PBE as $\omega \rightarrow \infty$. Although it has been shown to yield accurate band gaps, lattice constants, and bulk moduli in solids,[4−7] for example, it performs less well for molecular thermochemistry and reaction barriers due to the incorrect behavior of the exchange potential, HSE only includes a significant fraction of exact exchange for $r_{12} \leq 1/\omega \approx 4.8$ Å. On the basis of the long-range correction scheme of Iikura and co-workers,[24] the LC-ωPBE functional was introduced by Vydrov and Scuseria[8,9] to address this shortcoming and, opposite to HSE, exclusively contains Hartree−Fock exchange at large r_{12}. The LC-ωPBE energy is given by

$$E_{\mathrm{xc}}^{\mathrm{LC}-\omega\mathrm{PBE}} = E_{\mathrm{x}}^{\mathrm{PBE,SR}} + E_{\mathrm{x}}^{\mathrm{HF,LR}} + E_{\mathrm{c}}^{\mathrm{PBE}} \tag{3}$$

with the parameter $\omega = 0.4\ a_0^{-1}$ ($r_{12} \approx 1.3$ Å). Note that the Coulomb-attenuated method (CAM) functionals of Yanai and co-workers[25] had previously been introduced to achieve a similar goal. CAM-B3LYP, for example, yields hugely improved charge transfer excitations as compared to B3LYP but differs from the LC hybrid functionals in that it still contains a small fraction of exact exchange at small r_{12}. While LC-ωPBE improves upon HSE for a number of molecular properties, the inclusion of long-range exact exchange makes the functional unsuitable for calculations on solids. The motivation for the development of the HISS (Henderson−Izmaylov−Scuseria−Savin) functional[10] was to introduce a functional that benefits from the increased accuracy afforded by including exact exchange at long-range, but that is still suitable for studies of extended systems. In the HISS functional, the Coulomb operator is split into three length ranges:

$$\frac{1}{r_{12}} = \underbrace{\frac{\mathrm{erfc}(\omega_{\mathrm{SR}} r_{12})}{r_{12}}}_{\mathrm{SR}} + \underbrace{\frac{\mathrm{erfc}(\omega_{\mathrm{LR}} r_{12}) - \mathrm{erfc}(\omega_{\mathrm{SR}} r_{12})}{r_{12}}}_{\mathrm{MR}} + \underbrace{\frac{\mathrm{erf}(\omega_{\mathrm{LR}} r_{12})}{r_{12}}}_{\mathrm{LR}} \tag{4}$$

where MR denotes the additional middle-range length scale. As for HSE, exact exchange contributions for large r_{12} must be neglected to ensure the applicability of the functional to solids, but as in LC-ωPBE, short-range exact exchange is also omitted. That is, HISS contains exact exchange only in the middle range. Thus, we can write the total HISS exchange-correlation energy as

$$E_{xc}^{HISS} = E_{xc}^{PBE} + \frac{3}{5}(E_x^{HF,MR} - E_x^{PBE,MR}) \quad (5)$$

where the mixing coefficient 3/5 has been shown to be thermochemically optimal. The definition of a third range requires two values of the parameter ω, which have been determined as $\omega_{SR} = 0.84\ a_0^{-1}$ ($r_{12} \approx 0.6$ Å) and $\omega_{LR} = 0.20\ a_0^{-1}$ ($\sim$2.6 Å). Note that both HSE and LC-ωPBE are special cases of HISS-type functionals and can be defined within the framework of a three-range Coulomb operator with appropriate parameters.

2.2. Empirical Dispersion Corrections. Following the prescription of Grimme,[12] the DFT-D energy can be written as

$$E_{DFT-D} = E_{DFT} + E_{disp} \quad (6)$$

For an N-atom system, E_{disp} is defined as the simple pairwise sum:

$$E_{disp} = -s_6 \frac{1}{2} \sum_{i \neq j} \frac{C_6^{ij}}{R_{ij}^6} f(R_{ij}) \quad (7)$$

where s_6 is the global scaling parameter, which depends only on the functional in use, C_6^{ij} is the geometric mean of the individual atomic dispersion coefficients, R_{ij} is interatomic distance for a given pair, and f is the damping function:

$$f = \frac{1}{1 + \exp\left[-d\left(\frac{R_{ij}}{R_r} - 1\right)\right]} \quad (8)$$

where R_r is the sum of van der Waals radii for a given pair. Accurate dispersion coefficients and careful damping ($d = 20$ has been shown to be optimal)[13] are vital to ensure the correction applies only to medium-range R_{ij}, where the dispersion forces are greatest. The derivatives $\partial E_{disp}/\partial R_{ij}$ and $\partial^2 E_{disp}/\partial R_{ij}^2$ are straightforward to determine and implement, enabling DFT-D geometry optimizations and frequency calculations to be performed for gas-phase molecules.

The DFT-D energy expression can be modified for extended systems by adding a sum over lattice vectors; then a correction to E_{DFT-D}, taking periodic boundary conditions (PBC) into account, can be computed as

$$E_{DFT-D}^{PBC} = E_{DFT} + E_{disp}^{g=0} - \frac{s_6}{2} \sum_{i=1}^{N} \sum_{g \neq 0} \sum_{j=1}^{N} \frac{C_6^{ij}}{R_{ij,g}^6} f(R_{ij,g}) \quad (9)$$

The term $E_{disp}^{g=0}$ is the dispersion interaction between atoms in the unit cell, while the final term is calculated between atoms i in the unit cell with atoms j in the image cells, where the image cells are generated by integer multiples g of each lattice vector and the factor of 1/2 is to avoid double counting. The gradient of the PBC dispersion energy has also been derived and implemented and is rendered only slightly more complicated than for the molecular case because of the need to determine the derivatives with respect to lattice vectors as well as atoms.[26]

There are previous reports of DFT-D for periodic systems in the literature. In one of the earliest such implementations, Ortmann et al.[15] performed periodic DFT-D calculations using plane-wave basis sets, with the PW91-D functional yielding mixed results for a wide variety of weakly bound systems. More recently, Kerber et al.[16] obtained accurate results for the interlayer spacing and binding energy in graphite and vanadia, as well as good reaction energies for the adsorption of organic molecules on silica and zeolites using the PBE-D functional. In addition, the B3LYP- D* functional of Civalleri et al.[17] has been shown to give good structural and energetic data for a representative set of molecular crystals. This empirically corrected functional is not quite the same as the B3LYP-D functional as defined within the framework of Grimme, as the atomic van der Waals radii are scaled instead of the entire dispersion correction. That is, s_6 in eqs 7 and 9 is equal to unity, but the van der Waals radii R_r in eq 8 are multiplied by a parameter s_R (equal to 1.3 for hydrogen and 1.05 for heavy atoms). This is similar to the approach of Jurečka et al.[27] except that they use a single value of s_R, optimized for each functional and basis set combination, for the whole periodic table.

Unlike the implementation of Civalleri et al., we do not have a fixed distance-based cutoff, but rather add contributions to E_{disp} from ever larger shells of matter until some convergence criterion κ is reached. This approach was chosen due to the unexpectedly long-range of non-negligible dispersion contributions found during testing, and the strong system dependence of such a cutoff. Typically, $\kappa = 10^{-10}\ E_h$ was used for both the energy and the gradient. This is tighter than is strictly necessary as this far exceeds the accuracy of the DFT quadrature, for example, but guarantees the smoothness of our DFT-D potential energy surfaces.

3. Computational Details

All calculations were performed using a development version of the Gaussian electronic structure program.[28] A number of basis sets were considered for use in this work. After our initial tests, we chose to use the def2-TZVPP basis sets[29] for the PBC calculations, whereas for the dimer calculations the aug-cc-pVQZ basis set was selected for Ne[30] and Kr,[31] while the aug-cc-pV(Q+d)Z[32] and aug-cc-pVQZ-PP[33] basis sets were used for Ar and Xe, respectively. These basis sets were used in conjunction with the small-core pseudopotential of Peterson et al.[33] for xenon in the solid and molecular calculations. For the parametrizations, the 6-311++G(3df,3pd) basis set[34] was used. Because the DFT-D method is best used with large, flexible basis sets,[12] this basis set was chosen to ensure the transferability of our parametrization while enabling the requisite SCF calculations to be performed in reasonable time. The counterpoise correction of Boys and Bernardi[35] was not computed for any of the systems studied, as basis set superposition errors for these systems have previously been shown to be very small with triple- or quadruple-ζ basis sets.[36] Tight and very tight convergence criteria were used throughout, for the SCF procedure and geometry optimizations, respectively. Furthermore, it was found during the initial stages of this work that very dense integration grids must be employed to achieve sufficiently accurate results for both the solid and the molecular

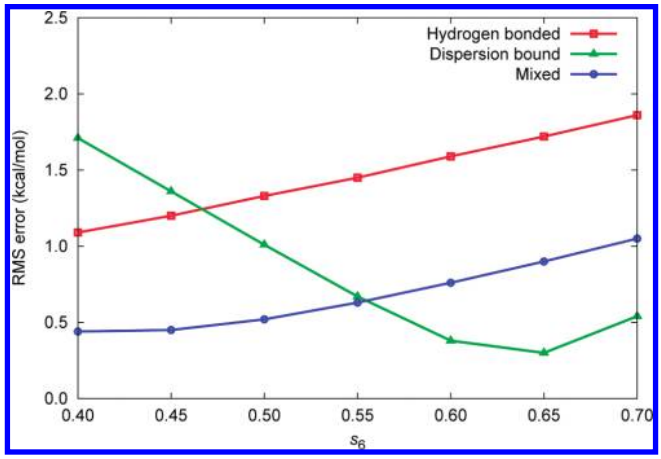

Figure 1. Plot of the rms errors in the HSE/6-311++G(3df,3pd) interaction energies for each type of complex in the S22 set against s_6, the global DFT-D scaling parameter.

calculations (especially the latter), and a grid with 199 radial and 974 angular points per atom was selected (for comparison, the "ultrafine" grid in Gaussian is a pruned grid with 99 radial and 590 angular points). This point is discussed further in section 5, as the choice of integration grid was found to have a significant effect, especially on some of the harmonic frequency calculations.

Although the main focus of this work was to evaluate the performance of the screened hybrid functionals HSE and HISS combined with an empirical dispersion correction, a number of other functionals were selected for comparison. In addition to BLYP,[37−39] PBE,[40] and TPSS[41] (both with and without the empirical correction), the M06-L functional[42] of Zhao et al. and Grimme's B97-D functional[13] were also selected. Of all of the recent Minnesota functionals, M06-L was chosen as it does not contain any nonlocal exchange, making it suitable for calculations on solids as well as molecules.[43]

4. Parametrization

As noted above, eq 7 contains one adjustable parameter, s_6, which depends only on the functional being used. Optimal values for this parameter have been determined for a number of popular functionals, but not for the screened functionals under consideration here. We determined the optimal s_6 values for the HSE and HISS functionals by minimizing the root-mean-square (rms) error of the interaction energies in the S22 set of molecular complexes. The S22 test set was proposed by Jurečka et al.[44] and contains three types of complex: hydrogen bonded (7 complexes), dispersion bound (8), and mixed (7). During the validation of our parametrization on functionals for which the optimized s_6 value has been determined, it was observed that DFT-D can degrade the performance of a given functional for hydrogen-bonded systems. In other words, the most accurate DFT-D interaction energies for these complexes are obtained when $s_6 = 0$ for a number of functionals; we note that this issue influenced the parametrization procedure of Jurečka and co-workers.[27] The need for a balanced test set is illustrated in Figure 1 by the rms interaction energy errors for each type of complex in the S22 set, calculated with the HSE functional and graphed against s_6, which clearly shows that simply minimizing the error for the dispersion bound subset would result in significantly larger errors for the other types of complexes.

Table 1. The rms Errors in the Interaction Energy (kcal/mol) in the S22 Set Calculated Using the HSE and HISS Functionals and the 6-311++G(3df,3pd) Basis Set, Both With and Without an Empirical Dispersion Correction

	HSE		HISS	
	DFT	DFT-D	DFT	DFT-D
hydrogen bonded	0.78	1.45	1.63	0.62
dispersion bound	4.56	0.67	4.38	0.48
mixed	1.46	0.63	1.52	0.65
overall	2.90	0.98	2.92	0.58

For both HSE and HISS, the optimal value of s_6 was determined to be 0.55. Table 1 shows the rms errors of the interaction energies for the S22 set complexes calculated with both functionals, with and without the empirical dispersion correction, and demonstrates the marked improvement of DFT-D for dispersion bound and mixed complexes. It is interesting to note that, while the increase in accuracy observed with HSE-D is a trade-off (because the errors for hydrogen-bonded systems increase), the addition of an empirical correction to HISS results in a uniform improvement for each type of complex. This suggests, prior to any detailed testing, that HISS-D in particular should provide good results across a range of weakly bound systems.

5. Applications

To assess the performance of DFT-D methods and especially the new HSE-D and HISS-D functionals for dispersion bound systems, we calculated the bond lengths (Table 2), harmonic frequencies (Tables 3 and 4), and dissociation energies (Table 5) of the rare gas dimers Ne_2, Ar_2, Kr_2, Xe_2, NeAr, NeKr, NeXe, ArKr, ArXe, and KrXe using the functionals stated above. The same methods were then used to calculate the lattice constants (Table 6), sublimation energies (Table 7), and band gaps Table 8) for the face-centered cubic structures of solid Ne, Ar, Kr, and Xe. These systems were chosen because, in addition to being bound solely by dispersion forces, they are quite different from those included in the parametrization; the S22 set features complexes of molecules containing only the atoms H, C, N, and O. Helium was excluded from our study as it does not exist as a solid at standard pressures, and our principal aim in this work is to demonstrate the applicability of HSE-D and HISS-D for both solid and molecular calculations.

For the dimers, we compare our calculated results to the experimental values of both Ogilvie and Wang[45,46] (OW) and Tang and Toennies[47] (TT) (note that these potentials are experimental in the sense that they are fits to experimental and not theoretical data). Although there is little difference between the two for equilibrium properties, the more recent TT potentials have been championed by Gerber and Ángyán,[48] and Ruzsinszky et al.[49] have recently shown that the OW potentials are actually divergent at large interatomic separation. Nonetheless, the OW potentials have been widely used as reference values in a number of theoretical studies, including the recent DFT investigations of Tao and Perdew[36]

Table 2. Equilibrium Bond Lengths of the Rare Gas Dimers (Å) Calculated Using the aug-cc-pVQZ Basis Sets

	Ne_2	Ar_2	Kr_2	Xe_2	NeAr	NeKr	NeXe	ArKr	ArXe	KrXe
HISS	3.4192	4.3244	4.6180	4.9450	3.8829	4.0590	4.3008	4.4798	4.6817	4.7957
HSE	3.1020	4.0254	4.3677	4.7805	3.5737	3.7604	3.9919	4.1980	4.4184	4.5836
M06-L	3.1496	3.9659	4.3836	4.9129	3.5618	3.8197	4.0143	4.2457	4.5086	4.7283
PBE	3.0880	3.9958	4.3459	4.7526	3.5420	3.7222	3.9409	4.1729	4.3885	4.5545
TPSS	3.3188	4.2698	4.6568	5.1624	3.7857	3.9770	4.2230	4.4713	4.7181	4.9057
B97D	3.2786	4.0428	4.1488	4.3772	3.6768	3.7832	3.9524	4.1003	4.2377	4.2729
BLYP-D	2.9327	3.8766	4.0664	4.3765	3.4222	3.5473	3.7413	3.9745	4.1472	4.2272
HISS-D	3.1196	3.9406	4.1216	4.3896	3.5495	3.6720	3.8600	4.0384	4.1984	4.2655
HSE-D	2.9312	3.8053	4.0545	4.3593	3.3818	3.5339	3.7353	3.9377	4.1179	4.2168
PBE-D	2.9004	3.7444	3.9891	4.3015	3.3300	3.4713	3.6585	3.8721	4.0459	4.1516
TPSS-D	3.0016	3.8607	4.0685	4.3429	3.4441	3.5759	3.7637	3.9735	4.1401	4.2152
OW[a]	3.0910	3.7565	4.0080	4.3627	3.4889	3.6210	3.8610	3.8810	4.0668	4.1740
TT[b]	3.0904	3.7572	4.0112	4.3657	3.4767	3.6460	3.8895	3.8895	4.0905	4.1964

[a] References 45 and 46. [b] Reference 47.

Table 3. Harmonic Frequencies of the Rare Gas Dimers (cm^{-1}) Calculated Using the aug-cc-pVQZ Basis Sets

	Ne_2	Ar_2	Kr_2	Xe_2	NeAr	NeKr	NeXe	ArKr	ArXe	KrXe
HISS	15.2	12.3	7.3	6.8	12.4	11.4	9.6	9.6	8.6	7.2
HSE	31.3	21.1	13.3	10.7	25.4	22.6	20.2	18.0	15.6	11.9
M06-L	77.8	47.8	33.3	23.8	46.6	53.2	47.9	35.2	28.8	28.0
PBE	33.9	22.8	15.1	11.6	28.5	25.3	23.9	19.0	17.6	13.5
TPSS	23.7	15.0	11.9	7.5	21.3	18.3	17.0	14.0	12.5	9.0
B97-D	31.0	22.6	21.7	23.7	29.1	25.8	26.5	23.7	24.1	23.2
BLYP-D	42.0	23.7	24.2	23.5	29.9	30.8	30.2	24.7	24.9	23.8
HISS-D	30.9	23.1	20.9	20.1	25.8	25.3	24.6	22.1	22.3	20.4
HSE-D	47.6	30.5	24.0	21.3	37.3	33.9	33.1	28.0	26.8	22.5
PBE-D	54.3	36.6	29.0	26.2	44.5	41.4	39.4	33.3	32.1	27.6
TPSS-D	43.7	30.4	24.8	23.6	36.3	34.1	32.8	27.8	26.7	24.1
OW[a]	28.5	30.9	23.6	20.9	28.2	26.2	24.3	27.9	27.1	22.7
TT[b]	29.4	32.0	24.3	21.2	28.5	25.3	22.8	28.7	26.9	22.7

[a] References 45 and 46. [b] Reference 47.

Table 4. Effect of the Integration Grid on the Harmonic Stretching Frequency of the Neon Dimer, Calculated at the TPSS/aug-cc-pVQZ Level With and Without the Boys−Bernardi Counterpoise Correction[a]

		ω_e (cm^{-1})	
grid	points per atom	without CP	with CP
pruned (75,302) "fine"	8338	46.5	46.7
pruned (99,590) "ultrafine"	23 416	41.2	34.3
(199,974)	167 528	23.7	23.5
(96,32,64)	169 984	44.8	35.8
(200,100,200)	3 440 000	25.2	23.6
(400,200,400)	27 520 000	25.6	24.5

[a] For notation, see the text.

and Zhao and Truhlar.[50] Errors are thus reported relative to the OW values, but generally the OW and TT potentials are in very close agreement for the properties studied here. We are also compelled to cite the highly accurate potentials of Aziz,[51,52] which were the preferred reference values of Ruzsinszky et al.[49] Finally, we note that the importance of the higher-order coefficients C_8 and C_{10} in the TT potentials has influenced the recent damped dispersion correction for GGA functionals of Steinmann et al.,[53] which appears to yield very promising results for a range of systems. However, these higher-order terms do not appear in the DFT-D framework of Grimme used in this work, although they have recently been derived from the exchange-hole dipole moment for the systems studied here by Becke and Johnson.[54]

Deviations from experimental values are reported as both mean signed errors (MSE) and mean unsigned errors (MUE) in Table 9 for the dimers and Table 11 for the solids. For the harmonic frequencies and dissociation energies of the dimers, these quantities are also expressed as percentages (see Table 10) because the experimental values are very small by chemical standards (dissociation energies are as low as 0.084 kcal/mol for Ne_2, rising to only 0.561 kcal/mol for Xe_2).

The uncorrected functional BLYP failed to bind any of the solids or dimers under investigation, and so results for this functional without an empirical dispersion correction are not tabulated in this section.

5.1. Dimers. *5.1.1. Bond Lengths.* Bond lengths for the rare gas dimers are given in Table 2. All of the DFT-D methods perform extremely well, and it is clear that the empirical correction is a necessity to obtain accurate geometries for these systems. Given the failure of its parent functional to bind any of the dimers at all, the accuracy of BLYP-D is especially pleasing. Without the dispersion correction PBE is the best functional, while HISS and TPSS give particularly large errors, but every uncorrected functional significantly overestimates the bond lengths in these dimers as shown by their positive mean signed errors in Table 9.

5.1.2. Harmonic Frequencies. The harmonic frequencies are listed in Table 3. B97-D is clearly the best performing functional here, with HISS-D, HSE-D, BLYP-D, and TPSS-D following close together. The empirical correction improves the results for HISS much more than for HSE, and this

Table 5. Dissociation Energies of the Rare Gas Dimers (kcal/mol) Calculated Using the aug-cc-pVQZ Basis Sets

	Ne_2	Ar_2	Kr_2	Xe_2	NeAr	NeKr	NeXe	ArKr	ArXe	KrXe
HISS	0.025	0.032	0.044	0.057	0.028	0.030	0.031	0.037	0.040	0.049
HSE	0.084	0.108	0.124	0.143	0.094	0.096	0.099	0.115	0.120	0.132
M06-L	0.162	0.142	0.103	0.136	0.171	0.167	0.193	0.129	0.144	0.122
PBE	0.122	0.145	0.163	0.181	0.135	0.140	0.145	0.153	0.158	0.171
TPSS	0.070	0.075	0.086	0.087	0.075	0.079	0.080	0.080	0.080	0.087
B97-D	0.146	0.255	0.493	0.825	0.186	0.239	0.276	0.349	0.427	0.626
BLYP-D	0.073	0.087	0.282	0.508	0.071	0.119	0.146	0.165	0.218	0.374
HISS-D	0.096	0.159	0.288	0.472	0.116	0.145	0.163	0.211	0.255	0.362
HSE-D	0.195	0.278	0.412	0.593	0.221	0.252	0.273	0.333	0.380	0.485
PBE-D	0.279	0.393	0.586	0.835	0.321	0.371	0.409	0.473	0.542	0.689
TPSS-D	0.226	0.329	0.532	0.793	0.263	0.314	0.348	0.412	0.477	0.638
OW[a]	0.084	0.285	0.400	0.561	0.134	0.142	0.147	0.361	0.375	0.464
TT[b]	0.084	0.285	0.400	0.562	0.132	0.141	0.141	0.333	0.373	0.464

[a] References 45 and 46. [b] Reference 47.

Table 6. Lattice Constants of the Rare Gas Solids (Å) Calculated with the def2-TZVPP Basis Set

	Ne	Ar	Kr	Xe
HISS	4.4574	5.8372	6.3487	6.9689
HSE	4.3768	5.7486	6.2896	6.9561
M06-L	4.2347	5.2605	5.5465	6.0045
PBE	4.3507	5.7436	6.3108	6.9978
TPSS	4.5523	6.1456	6.8171	7.6287
B97-D	4.4574	5.6027	5.7183	6.0507
BLYP-D	4.0464	5.2665	5.5808	6.0296
HISS-D	4.2214	5.3789	5.6688	6.0481
HSE-D	4.1604	5.3732	5.7123	6.1142
PBE-D	4.1203	5.2967	5.6271	6.0468
TPSS-D	4.2315	5.4354	5.6604	5.9807
expt.	4.464[a]	5.311[b]	5.67[c]	6.132[d]

[a] Reference 58. [b] Reference 59. [c] Reference 60. [d] Reference 61.

Table 7. Sublimation Energies of the Rare Gas Solids (J/mol) Calculated with the def2-TZVPP Basis Set

	Ne	Ar	Kr	Xe
HISS	2044	1332	1334	1319
HSE	2959	2459	2472	2497
M06-L	8471	11 119	12 640	20 192
PBE	4281	3120	2943	2842
TPSS	2834	1721	1509	1343
B97-D	6140	7928	14 687	25 462
BLYP-D	7533	7043	13 188	20 753
HISS-D	5054	6178	10 030	15 376
HSE-D	6270	7466	10 947	15 493
PBE-D	8988	10 298	15 112	21 536
TPSS-D	7918	8991	14 729	23 012
expt.	1933[a]	7732[b]	11 158[b]	15 839[b]

[a] Reference 62. [b] Reference 63.

Table 8. Band Gaps of the Rare Gas Solids (eV) Calculated with the def2-TZVPP Basis Set

	Ne	Ar	Kr	Xe
HISS	26.89	20.30	16.58	13.35
HSE	22.82	16.98	13.76	10.77
M06-L	21.29	16.75	12.60	8.43
PBE	19.43	15.06	12.22	9.57
TPSS	21.72	16.27	12.63	10.35
B97-D	21.01	15.39	11.90	8.16
BLYP-D	16.79	14.78	11.20	7.96
HISS-D	24.85	20.15	15.99	11.71
HSE-D	20.98	16.94	13.22	9.32
PBE-D	17.52	14.97	11.46	8.01
TPSS-D	19.10	15.70	12.14	8.46
expt.[a]	21.56	15.76	14.00	12.13

[a] Reference 64.

Table 9. Errors in the Bond Lengths, Harmonic Frequencies, and Dissociation Energies of the 10 Rare Gas Dimers Studied[a]

	r_e (Å)		ω_e (cm^{-1})		D_e (kcal/mol)	
	MSE	MUE	MSE	MUE	MSE	MUE
HISS	0.5196	0.5196	−16.0	16.0	−0.258	0.258
HSE	0.2491	0.2491	−7.0	7.6	−0.184	0.184
M06-L	0.2980	0.2980	16.2	16.2	−0.148	0.185
PBE	0.2192	0.2198	−4.9	6.1	−0.144	0.152
TPSS	0.5178	0.5178	−11.0	11.0	−0.215	0.215
B97-D	0.1560	0.1560	−0.9	2.7	0.087	0.095
BLYP-D	0.0001	0.0838	1.7	4.3	−0.091	0.091
HISS-D	0.0844	0.0846	−2.5	3.0	−0.069	0.075
HSE-D	−0.0237	0.0729	4.5	4.6	0.047	0.054
PBE-D	−0.0846	0.0846	10.4	10.4	0.195	0.195
TPSS-D	0.0075	0.0668	4.4	4.6	0.138	0.138

[a] Errors are given relative to the experimental results of Ogilvie and Wang.

appears to be due to the poor quality of the HSE-D frequencies for neon-containing dimers. Indeed, if only the Ar, Kr, and Xe dimers are considered, the accuracy of the HSE-D frequencies is spectacular (with a MSE and MUE equal to 0.0 and 0.3 cm^{-1}, respectively). Conversely, for the uncorrected HISS and HSE functionals, the errors in the calculated homonuclear dimer frequencies are far larger for the heavier elements. Of course, the effect of the empirical correction is most pronounced for the BLYP functional, with BLYP-D once again giving very good results here. The errors observed with the M06-L functional are surprisingly large, with the neon dimer proving especially troublesome.

We note that our frequencies differ significantly from those reported by Tao and Perdew,[36] who investigated the He, Ne, Ar, and Kr dimers using the LSDA, PBE, and TPSS functionals. Although we used the same basis set (except for Ar), there is a substantial discrepancy between some of our numbers, and this can be attributed solely to the choice of integration grid. We note that the need to use dense integration grids for GGA-type calculations on dispersion-bound systems has recently been highlighted and explained in great detail by Johnson et al.[55] The effects of using a larger grid, (199,974) in this work, are not uniform, but are especially pronounced in a few cases. Our value of ω_e for

Table 10. Percentage Errors in the Harmonic Frequencies and Dissociation Energies of the 10 Rare Gas Dimers Studied[a]

	ω_e		D_e	
	MSE	MUE	MSE	MUE
HISS	−62	62	−84	84
HSE	−28	30	−51	51
M06-L	60	60	−23	57
PBE	−20	24	−31	40
TPSS	−43	43	−63	63
B97-D	−2	10	37	40
BLYP-D	7	16	−30	30
HISS-D	−9	11	−17	22
HSE-D	17	17	36	38
PBE-D	39	39	97	97
TPSS-D	17	17	69	69

[a] For the harmonic frequencies, errors are given relative to the experimental results of Ogilvie and Wang as in Table 9.

Ne_2, calculated with TPSS, differs by 18.2 cm^{-1} from Tao and Perdew's value (over 60% of the experimental value). Focusing on this case, in particular, we chose to investigate this effect further by calculating ω_e with a variety of grids both with and without the counterpoise correction.[35] The results are tabulated in Table 4 and show that the grids usually used in benchmark calculations are inadequate in this case. The harmonic frequency calculated with the (199,974) grid used throughout this work agrees well with the value obtained with the (400,200,400) spherical product grid, with the latter containing 27.5 million points per atom. Note also that the magnitude of the basis set superposition error decreases with ever denser quadrature grids.

5.1.3. Dissociation Energies. Table 5 shows the dissociation energies for the 10 dimers considered here. All functionals yield significant errors in at least one case, but the best results are clearly obtained with the HISS-D functional. As for the harmonic frequencies, the effect of the dispersion correction here is varied and results in a far greater improvement for HISS than HSE, for example, and once more this seems to be due to the poor accuracy for the dimers containing neon. If these four dimers are excluded from the statistics, the HSE-D functional again yields astonishingly high accuracy (MSE of 0.006 kcal/mol, MUE equal to 0.017 kcal/mol). The effect of the correction on TPSS is limited, while it substantially degrades the PBE results.

5.1.4. Summary. Statistics for the bond lengths, harmonic frequencies, and dissociation energies of the dimers studied are given in Table 9.

The very nature of the interatomic force in these rare gas dimers makes them a challenging case for DFT methods. The recent study of Tao and Perdew,[36] as well as that of Zhao and Truhlar,[50] have demonstrated that, although geometries accurate to around 10% are within the reach of many functionals, calculating accurate dissociation energies is considerably more problematic. To assist with the analysis of the small values involved, mean percentage errors for both the dissociation energies and the harmonic frequencies are given in Table 10.

The DFT-D methods employed in this study yield excellent geometries and reasonable harmonic frequencies but struggle to provide accurate dissociation energies. For the frequencies, B97-D stands head and shoulders above every other functional, and for dissociation energies HISS-D comfortably outperforms all of the other methods. For both properties, HSE-D does extremely well in 6 out of 10 cases, but its performance is marred by its inaccurate results for the neon-containing dimers. It is worth mentioning that PBE performs reasonably well for each property, but it is clear that the best performers overall are B97-D and HISS-D, with the consistently accurate energetics of the latter especially pleasing.

5.2. Solids. *5.2.1. Lattice Constants.* Table 6 lists the calculated lattice constants for the fcc structures of solid neon, argon, krypton, and xenon. The lattice constants are very well reproduced by all DFT-D methods, as well as the uncorrected M06-L functional, and although there is little to choose between them, B97-D and HISS-D are the most accurate by a small margin.

5.2.2. Sublimation Energies. Shown in Table 7, the sublimation energies of the rare gas solids appear to provide a significant challenge for DFT methods. Of the functionals to which an empirical correction has not been added, only M06-L reproduces the trend of increasing ΔH_{sub} down the group. However, it significantly overestimates the values for neon, argon, and krypton. HISS is the only functional to yield an accurate value for neon, but given its performance for the other solids this may be purely fortuitous. All of the DFT-D methods correctly reproduce the periodic trend, but all hugely overestimate the sublimation energy of solid neon. Rościszewski et al.[56] and Acocella et al.[57] have performed detailed additivity studies of the sublimation energy of solid neon, and both groups find that the zero-point energy contributes approximately 30% of the experimental value (around 600 J/mol), but this is not sufficiently large to explain the discrepancies observed here. For argon, krypton, and xenon, HSE-D performs very well, with a mean unsigned error of only 274 J/mol (0.07 kcal/mol) for these three solids, or 1290 J/mol (0.31 kcal/mol) if neon is included. Note that, as for the thermochemistry of the dimers, the energies involved here are extremely small. HISS-D yields a value slightly closer to experiment for neon and performs well for both krypton and xenon, but underestimates the sublimation energy of argon.

5.2.3. Band Gaps. The band gaps of each solid, calculated as minimum direct band energy differences at the optimized geometry for each functional, are given in Table 8. HSE performs very well, but by contrast the HISS functional is the least accurate of those tested. This is surprising given that HISS has been shown to be only slightly less accurate that HSE for this property,[10] but it is worth noting that these solids have unusually large experimental band gaps and that all of the functionals give qualitatively correct results. The empirical dispersion correction results in a slight improvement for HISS but degrades the results for all other functionals. Although the DFT-D correction has no direct bearing on electronic structure, it is disappointing that the general improvement in geometry observed with the correction does not translate into more accurate band gaps. TPSS performs surprisingly well, especially for the lighter elements; likewise, the statistics for M06-L are skewed somewhat by

Table 11. Errors in the Lattice Constants, Sublimation Energies, and Band Gaps of the Rare Gas Solids Studied

	a (Å)		ΔH_{sub} (J/mol)		band gap (eV)	
	MSE	MUE	MSE	MUE	MSE	MUE
HISS	0.5088	0.5121	−7658	7714	3.42	3.42
HSE	0.4485	0.4921	−6569	7082	0.22	1.02
M06-L	−0.1327	0.1327	3940	3940	−1.09	1.59
PBE	0.4565	0.5131	−5869	7043	−1.79	1.79
TPSS	0.8917	0.8917	−7314	7764	−0.62	0.95
B97-D	0.0630	0.1070	4389	4389	−1.75	1.75
BLYP-D	−0.1634	0.1634	2964	3308	−3.18	3.18
HISS-D	−0.0650	0.0989	−6	1567	2.31	2.52
HSE-D	−0.0542	0.1064	879	1290	−0.75	1.34
PBE-D	−0.1215	0.1215	4818	4818	−2.87	2.87
TPSS-D	−0.0673	0.1295	4497	4497	−2.01	2.01

the larger errors for krypton and, especially, xenon. While more extensive testing is warranted, this indicates that the changes in geometry due to adding the correction are insufficient to alter the band gap, and thus a functional that is adequate for band gaps will be adequate after correction.

5.2.4. Summary. Statistics for the lattice constants, sublimation energies, and band gaps of the solids studied can be found in Table 11.

Generally, traditional functionals perform poorly for these systems. Lattice constants are generally overestimated, and sublimation energies are wildly inaccurate. M06-L is the best of the uncorrected functionals for both properties, yielding reasonable lattice constants and qualitatively correct sublimation energies and band gaps.

The empirical dispersion correction makes a substantial difference to the computed lattice constants and sublimation energies, although all DFT-D methods except B97-D underestimate the lattice constant for neon. This may, in part, explain the hugely overestimated DFT-D sublimation energies for neon, although the value of ΔH_{sub} obtained with B97-D is also poor. Aside from neon, the accuracy of the HSE-D and HISS-D sublimation energies is excellent. As expected, HSE yields accurate band gaps for all of these solids, with TPSS and M06-L also doing well. The empirical correction is purely a function of nuclear geometry and not electronic structure, however, so it can have only a limited effect on the band gap.

As with the dimers, no functional is the best performer for every property, but we would argue that, overall, HSE-D is the most consistent. For geometries and energetics, HISS-D gives good results but is somewhat less accurate for band gaps.

6. Conclusions

The screened hybrid functionals HSE and HISS have been extended with the addition of an empirical dispersion correction. Within Grimme's DFT-D framework, we find that setting the global scaling parameter s_6 to 0.55 for both functionals gives the best results. The HSE-D and HISS-D functionals have been evaluated through calculations on a number of rare gas dimers and solids. Both were found to perform very well overall, with HISS-D performing slightly better for the dimers and HSE-D having the edge for the solids, although if the four neon dimers are excluded from the statistics, HSE-D is also the best functional for the molecular calculations. Given the differences between the complexes used in the parametrization and the molecules and solids investigated in this work, we suggest that both HISS-D and HSE-D should be applicable to both molecular and extended systems in which exact exchange and dispersion play an important part.

Acknowledgment. We are grateful to Dr. Petr Jurečka for providing geometries for the S22 test set and for helpful discussions about DFT-D parametrization, and Dr. Tom Henderson for his comments on the manuscript. This work was supported by E.N.B.'s Texas A&M University at Qatar startup funds and NPRP 08-431-1-076 from the Qatar National Research Fund.

References

(1) Kohn, W.; Sham, L. J. *Phys. Rev.* **1965**, *140*, A1133.

(2) (a) Heyd, J.; Scuseria, G. E.; Ernzerhof, M. *J. Chem. Phys.* **2003**, *118*, 8207–8215. (b) Heyd, J.; Scuseria, G. E.; Ernzerhof, M. *J. Chem. Phys.* **2006**, *124*, 219906.

(3) Krukau, A. V.; Vydrov, O. A.; Izmaylov, A. F.; Scuseria, G. E. *J. Chem. Phys.* **2006**, *125*, 224106.

(4) Heyd, J.; Scuseria, G. E. *J. Chem. Phys.* **2004**, *121*, 1187–1192.

(5) Heyd, J.; Scuseria, G. E. *J. Chem. Phys.* **2004**, *120*, 7274–7280.

(6) Heyd, J.; Peralta, J. E.; Scuseria, G. E.; Martin, R. L. *J. Chem. Phys.* **2005**, *123*, 174101.

(7) Janesko, B. G.; Henderson, T. M.; Scuseria, G. E. *Phys. Chem. Chem. Phys.* **2009**, *11*, 443–454.

(8) Vydrov, O. A.; Heyd, J.; Krukau, A. V.; Scuseria, G. E. *J. Chem. Phys.* **2006**, *125*, 074106.

(9) Vydrov, O. A.; Scuseria, G. E. *J. Chem. Phys.* **2006**, *125*, 234109.

(10) Henderson, T. M.; Izmaylov, A. F.; Scuseria, G. E.; Savin, A. *J. Chem. Phys.* **2007**, *127*, 221103.

(11) Henderson, T. M.; Izmaylov, A. F.; Scuseria, G. E.; Savin, A. *J. Chem. Theory Comput.* **2008**, *4*, 1254–1262.

(12) Grimme, S. *J. Comput. Chem.* **2004**, *25*, 1463–1473.

(13) Grimme, S. *J. Comput. Chem.* **2006**, *27*, 1787–1799.

(14) Dobson, J. F.; White, A.; Rubio, A. *Phys. Rev. Lett.* **2006**, *96*, 073201−4.

(15) Ortmann, F.; Bechstedt, F.; Schmidt, W. G. *Phys. Rev. B* **2006**, *73*, 205101.

(16) Kerber, T.; Sierka, M.; Sauer, J. *J. Comput. Chem.* **2008**, *29*, 2088–2097.

(17) Civalleri, B.; Zicovich-Wilson, C. M.; Valenzano, L.; Ugliengo, P. *CrystEngComm* **2008**, *10*, 405–410.

(18) Henderson, T. M.; Janesko, B. G.; Scuseria, G. E. *J. Phys. Chem. A* **2008**, *112*, 12530–12542.

(19) Savin, A. In *Recent Developments and Applications of Modern Density Functional Theory*; Seminario, J. M., Ed.; Elsevier: Amsterdam, 1996; Chapter 9, pp 327−357.

(20) Toulouse, J.; Colonna, F.; Savin, A. *Phys. Rev. A* **2004**, *70*, 062505.

(21) Ernzerhof, M.; Scuseria, G. E. *J. Chem. Phys.* **1999**, *110*, 5029–5036.

(22) Zecca, L.; Gori-Giorgi, P.; Moroni, S.; Bachelet, G. B. *Phys. Rev. B* **2004**, *70*, 205127.

(23) Perdew, J. P.; Emzerhof, M.; Burke, K. *J. Chem. Phys.* **1996**, *105*, 9982–9985.

(24) Iikura, H.; Tsuneda, T.; Yanai, T.; Hirao, K. *J. Chem. Phys.* **2001**, *115*, 3540–3544.

(25) Yanai, T.; Tew, D. P.; Handy, N. C. *Chem. Phys. Lett.* **2004**, *393*, 51–57.

(26) Kudin, K. N.; Scuseria, G. E.; Schlegel, H. B. *J. Chem. Phys.* **2001**, *114*, 2919–2923.

(27) Jurečka, P.; Černý, J.; Hobza, P.; Salahub, D. R. *J. Comput. Chem.* **2007**, *28*, 555–569.

(28) Frisch, M. J.; Trucks, G. W.; Schlegel, H. B.; Scuseria, G. E.; Robb, M. A.; Cheeseman, J. R.; Scalmani, G.; Barone, V.; Mennucci, B.; Petersson, G. A.; Nakatsuji, H.; Caricato, M.; Li, X.; Hratchian, H. P.; Izmaylov, A. F.; Bloino, J.; Zheng, G.; Sonnenberg, J. L.; Hada, M.; Ehara, M.; Toyota, K.; Fukuda, R.; Hasegawa, J.; Ishida, M.; Nakajima, T.; Honda, Y.; Kitao, O.; Nakai, H.; Vreven, T.; Montgomery, J. A., Jr.; Peralta, J. E.; Ogliaro, F.; Bearpark, M.; Heyd, J. J.; Brothers, E.; Kudin, K. N.; Staroverov, V. N.; Kobayashi, R.; Normand, J.; Raghavachari, K.; Rendell, A.; Burant, J. C.; Iyengar, S. S.; Tomasi, J.; Cossi, M.; Rega, N.; Millam, J. M.; Klene, M.; Knox, J. E.; Cross, J. B.; Bakken, V.; Adamo, C.; Jaramillo, J.; Gomperts, R.; Stratmann, R. E.; Yazyev, O.; Austin, A. J.; Cammi, R.; Pomelli, C.; Ochterski, J. W.; Martin, R. L.; Morokuma, K.; Zakrzewski, V. G.; Voth, G. A.; Salvador, P.; Dannenberg, J. J.; Dapprich, S.; Parandekar, P. V.; Mayhall, N. J.; Daniels, A. D.; Farkas, O.; Foresman, J. B.; Ortiz, J. V.; Cioslowski, J.; Fox, D. J. *Gaussian Development Version*, revision H.01; Gaussian, Inc.: Wallingford, CT, 2009.

(29) Weigend, F.; Ahlrichs, R. *Phys. Chem. Chem. Phys.* **2005**, *7*, 3297–3305.

(30) Dunning, T. H. *J. Chem. Phys.* **1989**, *90*, 1007–1023.

(31) Wilson, A. K.; Woon, D. E.; Peterson, K. A.; Dunning, T. H. *J. Chem. Phys.* **1999**, *110*, 7667–7676.

(32) Dunning, T. H.; Peterson, K. A.; Wilson, A. K. *J. Chem. Phys.* **2001**, *114*, 9244–9253.

(33) Peterson, K. A.; Figgen, D.; Goll, E.; Stoll, H.; Dolg, M. *J. Chem. Phys.* **2003**, *119*, 11113–11123.

(34) Krishnan, R.; Binkley, J. S.; Seeger, R.; Pople, J. A. *J. Chem. Phys.* **1980**, *72*, 650–654.

(35) Boys, S. F.; Bernardi, F. *Mol. Phys.* **1970**, *19*, 553–566.

(36) Tao, J.; Perdew, J. P. *J. Chem. Phys.* **2005**, *122*, 114102–7.

(37) Becke, A. D. *Phys. Rev. A* **1988**, *38*, 3098.

(38) Lee, C.; Yang, W.; Parr, R. G. *Phys. Rev. B* **1988**, *37*, 785.

(39) Miehlich, B.; Savin, A.; Stoll, H.; Preuss, H. *Chem. Phys. Lett.* **1989**, *157*, 200–206.

(40) (a) Perdew, J. P.; Burke, K.; Ernzerhof, M. *Phys. Rev. Lett.* **1996**, *77*, 3865. (b) Perdew, J. P.; Burke, K.; Ernzerhof, M. *Phys. Rev. Lett.* **1997**, *78*, 1396 .

(41) Tao, J.; Perdew, J. P.; Staroverov, V. N.; Scuseria, G. E. *Phys. Rev. Lett.* **2003**, *91*, 146401.

(42) Zhao, Y.; Truhlar, D. G. *J. Chem. Phys.* **2006**, *125*, 194101–18.

(43) Zhao, Y.; Truhlar, D. G. *J. Chem. Phys.* **2009**, *130*, 074103.

(44) Jurečka, P.; Šponer, J.; Černý, J.; Hobza, P. *Phys. Chem. Chem. Phys.* **2006**, *8*, 1985–1993.

(45) Ogilvie, J. F.; Wang, F. Y. H. *J. Mol. Struct.* **1992**, *273*, 277–290.

(46) Ogilvie, J. F.; Wang, F. Y. H. *J. Mol. Struct.* **1993**, *291*, 313–322.

(47) Tang, K. T.; Toennies, J. P. *J. Chem. Phys.* **2003**, *118*, 4976–4983.

(48) Gerber, I. C.; Ángyán, J. G. *J. Chem. Phys.* **2007**, *126*, 044103.

(49) Ruzsinszky, A.; Perdew, J. P.; Csonka, G. I. *J. Phys. Chem. A* **2005**, *109*, 11015–11021.

(50) Zhao, Y.; Truhlar, D. G. *J. Phys. Chem. A* **2006**, *110*, 5121–5129.

(51) Aziz, R. A.; Slaman, M. *J. Chem. Phys.* **1989**, *130*, 187–194.

(52) Aziz, R. A. *J. Chem. Phys.* **1993**, *99*, 4518–4525.

(53) Steinmann, S. N.; Csonka, G.; Corminboeuf, C. *J. Chem. Theory Comput.* **2009**, *5*, 2950–2958.

(54) (a) Becke, A. D.; Johnson, E. R. *J. Chem. Phys.* **2006**, *124*, 014104−6. (b) Becke, A. D.; Johnson, E. R. *J. Chem. Phys.* **2007**, *127*, 154108–6.

(55) Johnson, E. R.; Becke, A. D.; Sherrill, C. D.; DiLabio, G. A. *J. Chem. Phys.* **2009**, *131*, 034111−7.

(56) Rościszewski, K.; Paulus, B.; Fulde, P.; Stoll, H. *Phys. Rev. B* **2000**, *62*, 5482.

(57) Acocella, D.; Horton, G. K.; Cowley, E. R. *Phys. Rev. B* **2000**, *61*, 8753.

(58) Batchelder, D. N.; Losee, D. L.; Simmons, R. O. *Phys. Rev.* **1967**, *162*, 767.

(59) Peterson, O. G.; Batchelder, D. N.; Simmons, R. O. *Phys. Rev.* **1966**, *150*, 703.

(60) Losee, D. L.; Simmons, R. O. *Phys. Rev.* **1968**, *172*, 944.

(61) Sears, D. R.; Klug, H. P. *J. Chem. Phys.* **1962**, *37*, 3002–3006.

(62) McConville, G. T. *J. Chem. Phys.* **1974**, *60*, 4093–4093.

(63) Schwalbe, L. A.; Crawford, R. K.; Chen, H. H.; Aziz, R. A. *J. Chem. Phys.* **1977**, *66*, 4493–4502.

(64) Magyar, R. J.; Fleszar, A.; Gross, E. K. U. *Phys. Rev. B* **2004**, *69*, 045111.

CT900536N